

Dissipative-coupling-induced magnomechanical chaos

Qin Wu(吴琴), Jiao Peng(彭椒), Yu-Dong Chen(陈毓东), and Zeng-Xing Liu(刘增星)
Citation: Chin. Phys. B, 2026, 35 (**3**): 037501. DOI: 10.1088/1674-1056/adfa7a
http://cpb.iphy.ac.cn; http://iopscience.iop.org/cpb

What follows is a list of articles you may be interested in

Temperature-dependent magnetotransport properties of $CoFe_2O_4$/Pt heterostructure

Haomang He(何浩茫), Ruijie Xu(徐睿劼), Anke Song(宋安柯), Zhongqiang Chen(陈中强), and Xuefeng Wang(王学锋)
Chin. Phys. B, 2026, 35 (**1**): 017502. DOI: 10.1088/1674-1056/ae181c

Effect of interlayer interaction on magnon properties of vdW honeycomb heterostructures

Jun Shan(单俊), Lichuan Zhang(张礼川), Huasu Fu(付华宿), Yuee Xie(谢月娥), Yuriy Mokrousov, and Yuanping Chen(陈元平)
Chin. Phys. B, 2025, 34 (**8**): 087501. DOI: 10.1088/1674-1056/adce97

Magnon behavior in YIG film under microwave excitation investigated by Brillouin light scattering

Guofu Xu(徐国服), Kang An(安康), Wenjun Ma(马文俊), Xiling Li(李喜玲), C. K. Ong, Chi Zhang(张驰), and Guozhi Chai(柴国志)
Chin. Phys. B, 2025, 34 (**6**): 067507. DOI: 10.1088/1674-1056/add24c

First- and second-order magnonic topologies in the ferromagnetic breathing SSH model modulated by non-Hermitian effects

Huasu Fu(付华宿), Lichuan Zhang(张礼川), Rami Mrad, Yuee Xie(谢月娥), and Yuanping Chen(陈元平)
Chin. Phys. B, 2025, 34 (**6**): 067506. DOI: 10.1088/1674-1056/addaa0

Strain-manipulated dispersion characteristics of magnonic crystals with Dzyaloshinskii-Moriya interaction and applications on spin-wave devices

Chuhan Zhou(周楚涵), Xiaotian Jiao(焦晓天), Jiaxi Xu(徐佳熙), Zhaonian Jin(金兆年), Lin Chen(陈琳), and Zhikuo Tao(陶志阔)
Chin. Phys. B, 2025, 34 (**2**): 027501. DOI: 10.1088/1674-1056/ad9892

Dissipative-coupling-induced magnomechanical chaos

Qin Wu(吴琴)[1,2,†], Jiao Peng(彭椒)[3], Yu-Dong Chen(陈毓东)[1], and Zeng-Xing Liu(刘增星)[3]

[1] *The First Dongguan Affiliated Hospital, Guangdong Medical University, Dongguan* 523808, *China*
[2] *School of Biomedical Engineering, Guangdong Medical University, Dongguan* 523808, *China*
[3] *School of Electronic Engineering & Intelligentization, Dongguan University of Technology, Dongguan* 523808, *China*

(Received 21 April 2025; revised manuscript received 11 August 2025; accepted manuscript online 12 August 2025)

Chaotic motion that exhibits extraordinary dynamic behavior has attracted particular attention in magnonics in the context of understanding nonlinear magnomechanical interaction. Here, we theoretically explore the magnomechanical chaos induced by dissipative coupling in an open cavity magnomechanical system. Numerical calculations of the magnomechanical dynamics show that the introduction of dissipative coupling can greatly enhance the nonlinearity of the system and induces ultra-low driving threshold chaotic motion, which effectively solves the bottleneck that the weak magnetostrictive interaction cannot trigger chaotic motion in a cavity magnomechanical system. Furthermore, we find that the degree of chaos represented by the Lyapunov exponent can be well tuned by changing the dissipative coupling strength. In addition to providing insight into chaotic behavior in open magnomechanical systems, dissipative-coupling-induced chaotic motion may also hold for other magnonic quantum systems since magnons possess excellent compatibility with other quasiparticles, and may find applications in the chaotic transfer of information.

Keywords: cavity magnomechanical system, magnetostrictive interaction, chaotic motion

PACS: 75.30.Ds, 75.80.+q, 05.45.–a, 05.45.Pq

DOI: 10.1088/1674-1056/adfa7a **CSTR:** 32038.14.CPB.adfa7a

1. Introduction

Magnonics, as an emergent interdisciplinary field, has been widely studied in the fields of condensed matter physics, quantum optics and spintronics.[1–4] Magnons, the quasiparticles of spin waves, serve as the information carrier that have no movement of charge during the transmission process, avoiding the emergence of Ohmic losses, which is the key advantage of magnonic devices compared with electrons.[1] In recent years, magnomechanical system has attracted much interest in the context of understanding nonlinear magnetostrictive interaction, providing a special platform for observing many intriguing classical and quantum phenomena,[5–26] ranging from entanglement and squeezing states of magnons[14–20] and the magnon Kerr effect[24] to the ground-state cooling of mechanical vibration mode[27–30] and the magnonic frequency combs based on magnetostrictive effect.[31–34] A typical magnomechanical system consists of a microwave cavity mode, a magnon mode, and a mechanical mode, in which the mechanical mode couple to the magnon mode through the magnetostrictive effect, which is the core of the magnomechanical system and the main source of nonlinearity.[35–40] Chaos, as a distinct nonlinear phenomenon,[41–44] holds significant importance in exploring the nonlinear properties of magnonics;[4] however, the weak magnetostrictive interaction of magnons presents a challenge for generating chaotic motion.[45,46]

Recently, the concept of dissipative coupling has attracted particular attention due to its rich fundamental physics, materials, devices, and potential practical applications, where the cavity and magnon modes interact with cooperative external damping.[47–59] Many exotic phenomena based on dissipative coupling in magnonic systems have been reported; for example, previous studies have demonstrated that the dissipative interaction can suppress magnon damping and thereby reduce the threshold for conventional magnon Kerr bistability.[58] For comparable parameters, for instance, the bistability threshold for dissipatively coupled systems is lower by a factor of about 5, which opens up new possibilities for the exploration of nonlinear phenomena in cavity magnonics.[57] Furthermore, ultra-wideband magnonic frequency comb generation can be implemented by introducing dissipative coupling in an open magnomechanical system. The total width of the magnonic comb in the robust plateau region can be up to ∼400 comb lines, which is much broader and flatter than that reported in the previous works.[59] The introduction of dissipative coupling allows the observation of weak nonlinear phenomena that could not be observed before, which has important scientific significance and practical value in the study of nonlinear cavity magnomechanics.

Inspired by these works, we propose an efficient mechanism to induce ultra-low threshold magnomechanical chaos by introducing dissipative coupling interplay in an open magnomechanical system. Our results suggest that the dissipative coupling between the cavity and magnon modes plays a crucial role in the dynamic evolution of the magnomechanical system

†Corresponding author. E-mail: wuqin@gdmu.edu.cn

© 2026 Chinese Physical Society and IOP Publishing Ltd. All rights, including for text and data mining, AI training, and similar technologies, are reserved.

and can significantly enhance the nonlinear magnetostrictive interaction.[35–37] A chaotic motion with an ultra-low drive threshold ($\sim$ nW) is obtained in the magnomechanical system, and the introduction of dissipative coupling adds a new degree of freedom to the manipulation of magnomechanical chaotic motion. Besides being of fundamental importance in chaotic dynamics, this work may have broad implications for many practical applications of secret information processing and communication based on magnonic devices.[60,61]

2. Physical model and methods

The physical model we consider is schematically illustrated in Fig. 1(a), in which a highly polished single crystal yttrium iron garnet sphere with a diameter of 1 mm is placed above the intersection of the microwave cavity and waveguide line. The microwave driving source with a central frequency $\omega_{\rm d}$ and a driving amplitude $\Omega_{\rm d}=\sqrt{\kappa_{a,{\rm e}}P_{\rm d}/\hbar\omega_{\rm d}}$ ($\kappa_{a,{\rm e}}$ the external coupling of the microwave cavity mode to the waveguide, $P_{\rm d}$ the power of the microwave driving field) is introduced into the microwave cavity to excite the magnon mode of the YIG sphere.[5] Simultaneously, a bias magnetic field with a strength of B_0 is applied to saturate the magnetization and control the frequency of the Kittel mode, i.e., $\omega_m=\gamma B_0$, where the gyromagnetic ratio $\gamma/2\pi=28$ GHz/T.[62] As shown in Fig. 1(b), the magnon excitation will cause varying magnetization due to the magnetostrictive effect, thereby introducing the deformation mode of the ferromagnetic crystal and facilitating its coupling with the Kittel mode.[5] This coupling interaction can be described by a radiation pressure-like Hamiltonian,[63] i.e., $H_{mb}=\hbar g_{mb}\hat{m}^\dagger\hat{m}(\hat{b}+\hat{b}^\dagger)$, where g_{mb} is the single magnon–phonon coupling strength, and $\hat{b}^\dagger$ ($\hat{b}$) and $\hat{m}^\dagger$ ($\hat{m}$) correspond to the creation (annihilation) operators of the phonon mode with frequency ω_b and magnon with frequency ω_m, respectively. The crossline-microwave circuit supports both the standing wave and the traveling wave, where the standing wave forms the cavity mode and contributes to coherent coupling between the magnon mode and the microwave cavity mode, while the traveling wave induces the dissipative coupling between the cavity mode and the magnon mode by radiating energy into an open environment.[47–49] Furthermore, the dissipative coupling strength can be changed by moving the position of the YIG sphere so that the dissipative coupling dominates.[51] As a consequence, the interaction Hamiltonian between the magnon and the cavity photon is given by $H_{ma}=\hbar(g_{ma}+{\rm i}\Gamma)(\hat{a}^\dagger\hat{m}+\hat{a}\hat{m}^\dagger)$, here $\hat{a}^\dagger$ ($\hat{a}$) is the boson creation (annihilation) operator of the cavity mode with the intrinsic frequency ω_a. g_{ma} represents the coherent coupling strength arising from magnetic dipole moment interaction, and Γ denotes the dissipative coupling strength between the magnon and microwave cavity modes through their common storage layer.[47] Therefore, the Hamiltonian of the whole system, which consists of the photon, magnon and phonon modes and their interactions, can be written as

$$\begin{aligned}H &= \hbar\omega_a\hat{a}^\dagger\hat{a}+\hbar\omega_m\hat{m}^\dagger\hat{m}+\hbar\omega_b\hat{b}^\dagger\hat{b}\\&\quad+\hbar g_{mb}\hat{m}^\dagger\hat{m}(\hat{b}+\hat{b}^\dagger)+\hbar(g_{ma}+{\rm i}\Gamma)(\hat{a}^\dagger\hat{m}+\hat{a}\hat{m}^\dagger)\\&\quad+\hbar\Omega_{\rm d}(\hat{a}^\dagger{\rm e}^{-{\rm i}\omega_{\rm d}t}+\hat{a}{\rm e}^{{\rm i}\omega_{\rm d}t}).\end{aligned}\tag{1}$$

In order to eliminate the time dependence of the microwave pump term, the system is placed in the rotating frame at the frequency $\omega_{\rm d}$ of the microwave driving field, that is, the unitary transformation $\boldsymbol{U}(t)=\exp(-{\rm i}\omega_{\rm d}\hat{m}^\dagger\hat{m}t)$ is adopted. Thus, the effective Hamiltonian of this non-Hermitian system can be written as

$$\begin{aligned}H_{\rm eff} &= \boldsymbol{U}(t)H\boldsymbol{U}^\dagger(t)-{\rm i}\hbar\boldsymbol{U}(t)\frac{\partial\boldsymbol{U}^\dagger(t)}{\partial t}\\&=\hbar\Delta_a\hat{a}^\dagger\hat{a}+\hbar\Delta_m\hat{m}^\dagger\hat{m}+\hbar\omega_b\hat{b}^\dagger\hat{b}+\hbar g_{mb}\hat{m}^\dagger\hat{m}(\hat{b}+\hat{b}^\dagger)\\&\quad+\hbar(g_{ma}+{\rm i}\Gamma)(\hat{a}^\dagger\hat{m}+\hat{a}\hat{m}^\dagger)+\hbar\Omega_{\rm d}(\hat{a}^\dagger+\hat{a}),\end{aligned}\tag{2}$$

where $\Delta_{a(m)}=\omega_{a(m)}-\omega_{\rm d}$ denotes the frequency detuning between the cavity mode (magnon mode) and the microwave pump field. Under the semiclassical approximation,[64] the operators of each mode are reduced to their average values, viz. $a(t)\equiv\hat{a}(t)$, $m(t)\equiv\hat{m}(t)$, and $b(t)\equiv\hat{b}(t)$. The evolution of the magnomechanical system can be described by the Heisenberg–Langevin equation, i.e., $\dot{o}={\rm i}/\hbar[H,o]$ ($o=a,m,b$), as follows:

$$\begin{aligned}\begin{pmatrix}\dot{a}\\ \dot{m}\\ \dot{b}\end{pmatrix} &= -{\rm i}\begin{pmatrix}\Delta_a-{\rm i}\kappa_a & g_{ma}+{\rm i}\Gamma & 0\\ g_{ma}+{\rm i}\Gamma & \Delta_m-{\rm i}\kappa_m & 0\\ 0 & 0 & 0\end{pmatrix}\mathfrak{R}\\&\quad-{\rm i}\begin{pmatrix}0 & 0 & 0\\ 0 & g_{mb}(b+b^\dagger) & 0\\ 0 & -{\rm i}g_{mb}m^\dagger & \omega_b-{\rm i}\kappa_b\end{pmatrix}\mathfrak{R}-{\rm i}\mho+\rho,\end{aligned}\tag{3}$$

where $\mathfrak{R}=(a,m,b)^{\rm T}$ and $\mho=(\Omega_{\rm d},0,0)^{\rm T}$. κ_a is the total microwave cavity loss rate that can be written as the sum of the loss rate associated with the input coupling ($\kappa_{a,{\rm e}}$) and the remaining loss rate ($\kappa_{a,{\rm i}}$), i.e., $\kappa_a=\kappa_{a,{\rm e}}+\kappa_{a,{\rm i}}$. κ_m and κ_b are the intrinsic dissipation for the magnon and phonon modes, respectively. $\rho=\left(\sqrt{\kappa_a}a_{\rm in}(t),\sqrt{\kappa_m}m_{\rm in}(t),\sqrt{\kappa_b}b_{\rm in}(t)\right)^{\rm T}$ represent the white noise terms of the corresponding modes, characterized by the temperature-dependent correlation functions[64]

$$\begin{aligned}\langle a_{\rm in}(t)a_{\rm in}^\dagger(t')\rangle &= [n_{{\rm th},a}(\omega_a)+1]\delta(t-t'),\\ \langle a_{\rm in}^\dagger(t)a_{\rm in}(t')\rangle &= [n_{{\rm th},a}(\omega_a)]\delta(t-t'),\\ \langle m_{\rm in}(t)m_{\rm in}^\dagger(t')\rangle &= [n_{{\rm th},m}(\omega_m)+1]\delta(t-t'),\\ \langle m_{\rm in}^\dagger(t)m_{\rm in}(t')\rangle &= [n_{{\rm th},m}(\omega_m)]\delta(t-t'),\\ \langle b_{\rm in}(t)b_{\rm in}^\dagger(t')\rangle &= [n_{{\rm th},b}(\omega_b)+1]\delta(t-t'),\\ \langle b_{\rm in}^\dagger(t)b_{\rm in}(t')\rangle &= [n_{{\rm th},b}(\omega_b)]\delta(t-t').\end{aligned}\tag{4}$$

The thermal occupancy of the baths is given by Bose–Einstein distributions, i.e.,

$$n_{{\rm th},(a,m)} = \frac{1}{\exp\left[\frac{\hbar\omega_{(a,m)}}{K_{\rm B}T_{\rm bath}}\right]-1},$$

$$n_{\mathrm{th},(b)} = \frac{1}{\exp\left[\frac{\hbar\omega_{(b)}}{K_{\mathrm{B}}T_{\mathrm{bath}}}\right]-1}, \tag{5}$$

where K_{B} is the Boltzmann constant and T_{bath} is the bath temperature (assumed to be the same for all the modes). Equation (3) is a set of nonlinear differential equations and thus the dissipative coupling between the magnon and microwave cavity modes will affect the dynamical evolution of the system, which may trigger some intriguing nonlinear phenomena.[47,48,58] In what follows, we discuss in detail the influence of dissipative coupling on the chaotic dynamics of the magnomechanical system. Firstly, to characterize the chaotic properties of the magnon, without loss of generality, we define the mean value of the magnon operator as $m = m_{\mathrm{r}} + \mathrm{i}m_{\mathrm{i}}$ (m_{r} and m_{i} are real numbers), and the intensity of the magnon is defined as $I_m = {m_{\mathrm{r}}}^2 + {m_{\mathrm{i}}}^2$. The magnonic spectrum $S(\omega)$ in the frequency domain can be obtained by performing the fast Fourier transform on I_m, where ω is the spectroscopic frequency. Furthermore, the chaotic system is extremely sensitive to tiny perturbations, and in order to quantitatively investigate such hypersensitivity to the initial conditions, we assume the evolution of a perturbation $\boldsymbol{\delta} = (\delta a_{\mathrm{r}}, \delta a_{\mathrm{i}}, \delta m_{\mathrm{r}}, \delta m_{\mathrm{i}}, \delta b_{\mathrm{r}}, \delta b_{\mathrm{i}})^{\mathrm{T}}$, which characterizes the divergence degree of adjacent trajectories in phase space.[41–43] Here, the perturbation components $\delta a_{\mathrm{r}}, \delta a_{\mathrm{i}}, \delta m_{\mathrm{r}}, \delta m_{\mathrm{i}}, \delta b_{\mathrm{r}}, \delta b_{\mathrm{i}}$ correspond to the quantum fluctuations of the respective mode operators around their classical mean-field values (e.g., $\delta a_{\mathrm{r}}, \delta a_{\mathrm{i}}$ for the microwave cavity mode, $\delta m_{\mathrm{r}}, \delta m_{\mathrm{i}}$ for the magnon mode, and $\delta b_{\mathrm{r}}, \delta b_{\mathrm{i}}$ for the phonon mode).

Thence, the perturbation equation of $\boldsymbol{\delta}$ can be obtained by linearizing Eq. (3) and $\mathrm{d}\boldsymbol{\delta}/\mathrm{d}t = M\boldsymbol{\delta}$, with the coefficient matrix

$$M = \begin{pmatrix} -\kappa_a & \Delta_a & \Gamma & g_{ma} & 0 & 0 \\ -\Delta_a & -\kappa_a & -g_{ma} & \Gamma & 0 & 0 \\ \Gamma & g_{ma} & -\kappa_m & \Delta_m + 2g_{mb}b & 2g_{mb}m_{\mathrm{i}} & 0 \\ -g_{ma} & \Gamma & -\Delta_m + 2g_{mb}b & -\kappa_m & -2g_{mb}m_{\mathrm{r}} & 0 \\ 0 & 0 & 0 & 0 & -\kappa_b & \omega_b \\ 0 & 0 & -2g_{mb}m_{\mathrm{r}} & -2g_{mb}m_{\mathrm{i}} & -\omega_b & -\kappa_b \end{pmatrix}. \tag{6}$$

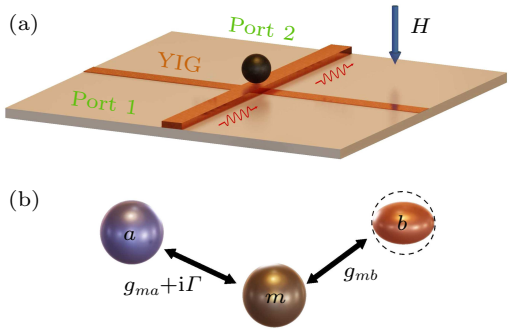


Fig. 1. (a) Schematic illustration of an open magnomechanical system, in which a yttrium iron garnet sphere is placed above the center of the crossline-microwave circuit that supports both the standing wave and the traveling wave. The YIG sphere is driven by a microwave pump source, which is input from port 1 or 2 and probed from the other port. A static bias magnetic field is applied along the depicted direction to saturate the magnetization. (b) Microscopic diagram of the interaction of three modes: the magnon mode is coupled with the microwave cavity mode (with the coupling strength $g_{ma} + \mathrm{i}\Gamma$) and the deformation mode (with the coupling strength g_{mb}), respectively.

The temporal evolution of the magnon mode can be obtained by numerically solving the nonlinear evolution Eq. (3) and the perturbation equations $\mathrm{d}\boldsymbol{\delta}/\mathrm{d}t = M\boldsymbol{\delta}$ under various initial conditions. To investigate the chaotic characteristics during the evolution process of magnomechanic dynamics, we take into account the evolution of a nearby point $(I_m + \delta I_m)$ of I_m to characterize the property of the magnon mode. The calculated exponential variation of δI_m ($\delta I_m = |m + \delta m|^2 - I_m$) demonstrates how the initial states of the cavity field evolve in the temporal domain and phase space. Note that the perturbation component δm corresponds to the quantum fluctuations of the magnon operator around the classical mean-field values (e.g., $\hat{m} \equiv m + \delta m$).

In what follows, we discuss the dynamic evolution of the magnomechanical system under dissipative coupling in detail. Figure 2 shows the numerical results of solving Eq. (3) and the perturbation equations $\mathrm{d}\boldsymbol{\delta}/\mathrm{d}t = M\boldsymbol{\delta}$ in the presence and absence of dissipative coupling. Specifically, in the absence of dissipative coupling i.e., $\Gamma/2\pi = 0$ MHz, the time evolution of the magnon number I_m is shown in Fig. 2(a). We can see that after a transient process, the oscillation of the magnon reaches a stable periodic oscillation before $t = 1$ μs. Note that the disordered oscillations in the inset of Fig. 2(a) arise from environmental white noise dominating the weak coherent dynamics under ultralow driving power ($P_{\mathrm{d}} = 1$ nW). The spectrum of the magnonic dynamics is shown in Fig. 2(c). It should be pointed out that the magnonic spectrum undergoes a frequency shift of ω_{d}, because the evolution equations describe the evolution of the magnon mode in a frame rotating at the driving frequency ω_{d}. Correspondingly, the exponentially decaying perturbation also demonstrates the periodic evolution of magnons [shown in Fig. 2(b)]. It can be seen from the above discussion that the chaotic motion of the magnomechanical system cannot be triggered by the weak nonlinear magnetostrictive interaction under a weak driving power. However, when dissipative coupling between the magnon and

microwave cavity modes is introduced ($\Gamma/2\pi = 20$ MHz), the magnon number I_m is dramatically enhanced by approximately 13 orders of magnitude [Fig. 2(d)]. This substantial amplification renders the influence of environmental thermal noise on the magnon dynamics negligible. At room temperature, the thermal magnon occupation number ($n_{\mathrm{th},m} \sim 10^3$) is far lower than the significantly boosted magnon population sustained by the dissipative coupling mechanism. Concurrently, the evolution of the perturbation δI_m exhibits exponential divergence over time [Fig. 2(e)], a hallmark signature of deterministic chaos.[42,43] In addition, the broadband spectrum [Fig. 2(f)] further corroborates chaos. This divergence signifies extreme sensitivity to initial conditions (the butterfly effect) and confirms the chaotic nature of the magnon dynamics under dissipative coupling, distinct from noise-induced fluctuations. Therefore, while environmental noise introduces minor fluctuations in the perturbation evolution trajectory and sideband spectrum under dissipative coupling, the defining chaotic characteristics of the system, such as a positive Lyapunov exponent, remain robustly present.

To further elucidate the pronounced dependency of magnomechanical chaos on dissipative coupling strength, we analyze the variation of the maximal Lyapunov exponent of the magnon mode with the dissipative coupling strength under the weak driving power $P_{\mathrm{d}} = 1$ nW. The maximal Lyapunov exponent of the magnon mode defined by the logarithmic slope of the perturbation δI_m, i.e., $\delta I_m(t) = \delta I_m(0)\,\mathrm{e}^{\lambda_{\mathrm{LE}} t}$, and the logarithmic slope, i.e.,

$$\lambda_{\mathrm{LE}} = \lim_{t\to\infty} \lim_{\delta I_m(0)\to 0} \frac{1}{t} \ln \left| \frac{\delta I_m(t)}{\delta I_m(0)} \right|, \tag{7}$$

which is a mensurable description of the rate of convergence or divergence of nearby trajectories in phase space. In physics, a positive Lyapunov exponent ($\lambda_{\mathrm{LE}} > 0$) implies that the evolution of the magnon mode is chaotic, i.e., divergence and sensitivity to initial conditions. Conversely, a negative Lyapunov exponent ($\lambda_{\mathrm{LE}} < 0$) indicates that the evolution of the magnon mode is ordered. In particular, a zero Lyapunov exponent ($\lambda_{\mathrm{LE}} = 0$) means that the appearance of period-doubling bifurcations.[41–43] Figure 3(a) shows the maximum Lyapunov exponent of the magnon mode varying with the dissipative coupling strength. Obviously, as the dissipative coupling strength increases, the Lyapunov exponent of the magnon mode changes from negative to positive, which means that the system enters a chaotic state from an ordered state. Furthermore, by adjusting the dissipative coupling strength, the degree of chaos can be effectively enhanced, which plays a crucial role in the chaotic behavior of the cavity magnomechanical system. It is worth noting that the dissipative coupling strength is controllable in experiments and can be adjusted by tuning the 3D position of the YIG sphere.[51] From the above results, it can be seen that dissipative coupling provides a feasible way to realize magnomechanical chaos under low power conditions. The variation of the Lyapunov exponent of the magnon mode with the intensity of the coherent coupling is also discussed, and the results are shown in the inset of Fig. 3(a). We can see that when the system is dominated by coherent coupling, the maximum Lyapunov exponent of the magnon is always negative as the coupling intensity increases, which means that coherent coupling cannot induce the system to enter chaotic motion under weak power drive. In this context, dissipative coupling provides a convincing alternative mechanism to address the severe challenge of being unable to trigger magnomechanical chaotic motion under weak driving.

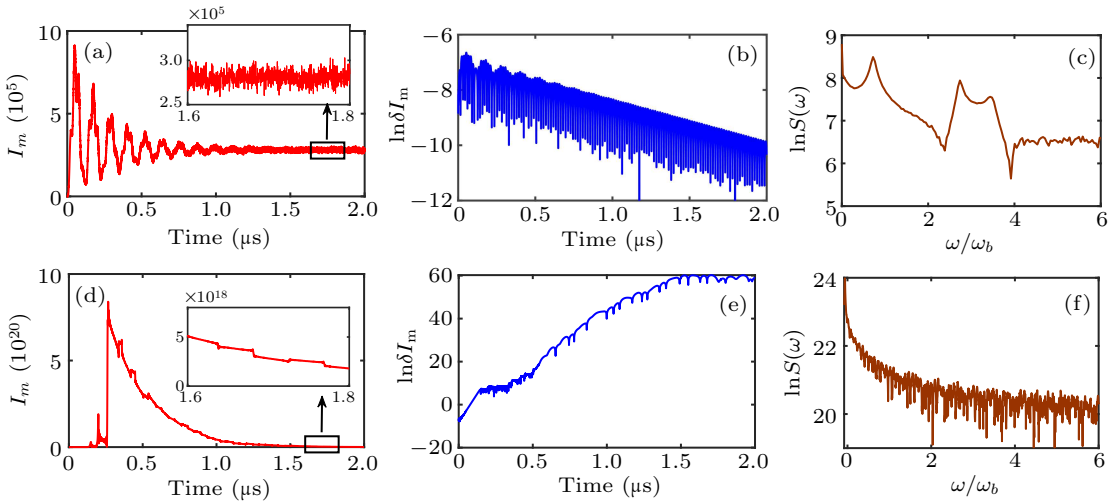


Fig. 2. (a) The time evolution of the magnon number I_m, (b) the temporal progression of perturbations $\ln \delta I_m$, and (c) the frequency spectrum output from the magnomechanical system $\ln S(\omega)$ are shown in the absence of the dissipative coupling $\Gamma/2\pi = 0$ MHz. Correspondingly, in the presence of the dissipative coupling, i.e., $\Gamma/2\pi = 20$ MHz, the results are shown in (d)–(f). The initial conditions are chosen as $a_{\mathrm{r}}|_{t=0} = a_{\mathrm{i}}|_{t=0} = b_{\mathrm{r}}|_{t=0} = b_{\mathrm{i}}|_{t=0} = m_{\mathrm{r}}|_{t=0} = m_{\mathrm{i}}|_{t=0} = 0$, and $\delta a_{\mathrm{r}}|_{t=0} = \delta a_{\mathrm{i}}|_{t=0} = \delta b_{\mathrm{r}}|_{t=0} = \delta b_{\mathrm{i}}|_{t=0} = \delta m_{\mathrm{r}}|_{t=0} = \delta m_{\mathrm{i}}|_{t=0} = 10^{-10}$. The parameters of this system have been selected based on the recent experiment:[5] $\omega_b/2\pi = 11.42$ MHz, $\kappa_{a,\mathrm{e}}/2\pi = \kappa_{a,\mathrm{i}}/2\pi = 1.67$ MHz, $\kappa_m/2\pi = 0.56$ MHz, $\kappa_b/2\pi = 150$ Hz, $g_{mb}/2\pi = 9.88$ mHz, $\Delta_a = \Delta_m = \omega_b$, the microwave driving field power $P_{\mathrm{d}} = 1$ nW and the bath temperature $T_{\mathrm{bath}} = 300$ K.

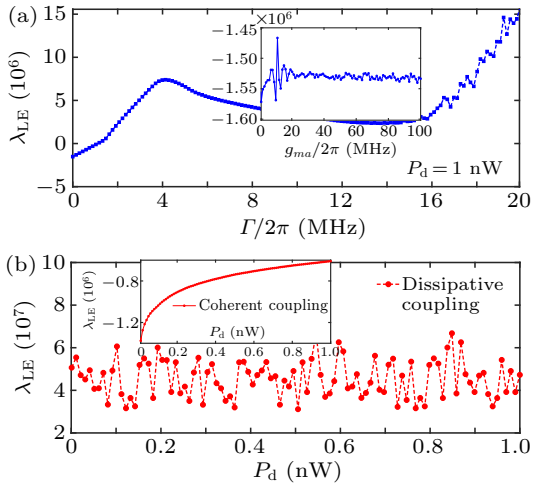


Fig. 3. (a) The maximum Lyapunov exponent of the magnon mode $\lambda_{\rm LE}$ versus the dissipative coupling strength $\Gamma/2\pi$ and the coherent coupling strength $g_{ma}/2\pi$ (the inset). The microwave drive field power is set to $P_{\rm d} = 1$ nW. (b) $\lambda_{\rm LE}$ as a function of the microwave driving power $P_{\rm d}$ under the dissipative coupling with $\Gamma/2\pi = 20$ MHz and the coherent coupling with $g_{ma}/2\pi = 20$ MHz (the inset). The other parameters are the same as those in Fig. 2.

A pivotal comparison of the maximal Lyapunov exponent $\lambda_{\rm LE}$ evolution with microwave driving power $P_{\rm d}$ under distinct coupling regimes: dissipative coupling ($\Gamma/2\pi = 20$ MHz) and coherent coupling ($g_{ma}/2\pi = 20$ MHz, the inset). Crucially, under dissipative coupling, $\lambda_{\rm LE}$ remains persistently positive ($\lambda_{\rm LE} > 0$) even at ultra-low driving powers down to $P_{\rm d} \ll 0.1$ nW. This signifies the emergence of chaotic dynamics effectively without a lower power threshold. In stark contrast, under coherent coupling, $\lambda_{\rm LE}$ remains strictly negative ($\lambda_{\rm LE} < 0$) even when $P_{\rm d}$ is increased by nine orders of magnitude up to 1 W, indicating only stable periodic oscillations. This profound difference stems from the distinct physical nature of the couplings. Dissipative coupling, mediated by interaction with a common reservoir (waveguide), introduces level attraction and significantly amplifies the magnon population.[47,48] This population boost dramatically enhances the effective nonlinearity arising from the magnetostrictive interaction, and the amplified nonlinearity readily triggers chaotic instability at minimal drive powers. Conversely, coherent coupling, while enabling energy exchange, lacks this inherent amplification mechanism. In addition, the effective damping rate of the magnon mode $\kappa_{\rm eff}$ is modified by the cavity-magnon interaction, i.e., $\kappa_{\rm eff} = \kappa_m + \eta\kappa_a$.[58] The coefficient $\eta = (g_{ma} + {\rm i}\Gamma)^2/(\Delta_a^2 + \kappa_a^2)$ stands for the transfer efficiency of the excitation power from the input port into the magnon system, and η is dependent on the frequency detuning Δ_a, and the total damping of the cavity κ_a. For the coherent coupling region ($\Gamma = 0$), in this case, $\eta = g_{ma}^2/(\Delta_a^2 + \kappa_a^2) > 0$, leading to an enhanced effective damping rate of the magnon mode, i.e., $\kappa_{\rm eff} = \kappa_m + \eta\kappa_a$. However, for the dissipative coupling region ($g_{ma} = 0$), in this case, $\eta = -\Gamma^2/(\Delta_a^2 + \kappa_a^2) < 0$, leading to a suppressed effective damping rate, i.e., $\kappa_{\rm eff} = \kappa_m - |\eta|\kappa_a$. Note that, in cavity magnonics, coherent and dissipative interactions usually coexist. Whereas, it is possible to design systems where one coupling type (coherent or dissipative) dominates. The choice to enhance or suppress certain interactions is guided by the objective of a specific device or experiment.[48]

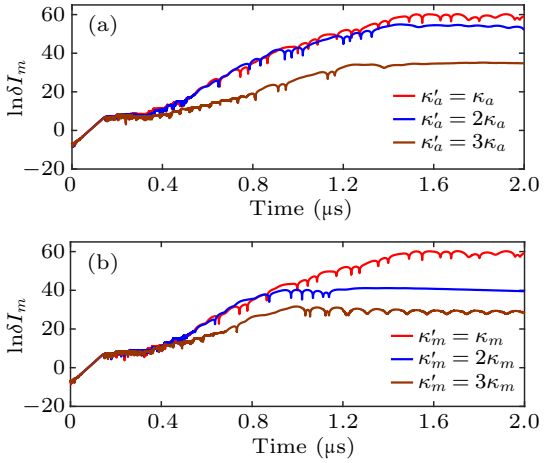


Fig. 4. Temporal evolution of the perturbation $\ln\delta I_m$ under different (a) cavity decay rates κ_a' and (b) magnon decay rates κ_m'. The other parameters are the same as those in Fig. 2.

It is worth noting that the dissipative magnon–photon interaction is mediated by mutual coupling of the magnon and cavity photon to a traveling-wave reservoir, which inevitably introduces additional dissipation in both the magnon mode κ_m' and the cavity mode κ_a'.[47,48,51] To comprehensively characterize the influence of additional dissipation on the chaotic dynamics, we present in Fig. 4 the detailed perturbation evolution δI_m under varying cavity and magnon dissipation rates. Phenomenologically, we add the additional dissipation to the evolution Eq. (3), and the Langevin equations are solved numerically with the same simulation parameters. The results show that magnomechanical chaos exhibits significant sensitivity to additional dissipation. To be specific, as the cavity additional dissipation increases (e.g., red curve: $\kappa_a' = \kappa_a$; blue curve: $\kappa_a' = 2\kappa_a$; brown curve: $\kappa_a' = 3\kappa_a$), the duration of the chaotic motion significantly diminishes (from ~ 1.6 μs to ~ 1.4 μs and shorter), accompanied by a reduction in the maximal Lyapunov exponent $\lambda_{\rm LE}$, indicating a suppression in both the persistence and the intensity of chaos. A qualitatively similar suppression of chaotic dynamics, characterized by reduced duration and $\lambda_{\rm LE}$, is observed upon increasing the additional magnon dissipation κ_m', as shown in Fig. 4(b). Physically, additional dissipation accelerates the energy loss from the coupled magnon–photon–phonon system, impeding the efficient buildup of nonlinear magnetostrictive interactions essential for chaotic instability. The faster energy decay curtails the time available for trajectories to diverge exponentially in phase space (shorter chaos duration) and dampens the amplification rate of initial perturbations (smaller $\lambda_{\rm LE}$). Consequently, achieving and maintaining the chaotic

state necessitates a careful trade-off between the nonlinearity-enhancing dissipative coupling and the chaos-suppressing environmental dissipation. These findings provide crucial theoretical guidance for the experimental realization and manipulation of ultra-low-threshold magnomechanical chaos. Furthermore, it should be pointed out that dissipative magnon-photon coupling inevitably introduces additional dissipation into both the magnon mode and the cavity mode. However, given that chaos is fundamentally a classical phenomenon, introducing gain into the cavity can compensate for this additional dissipation,[65,66] thereby enabling ultra-low-threshold chaos.

Finally, discuss the feasibility of the experimental realization of cavity magnomechanical chaos. First, the proposed system is simple and has high feasibility in experimental implementations. The dissipative coupling between the magnons and microwave photons has been experimentally demonstrated, and the parameter requirements are benchmarked against existing cavity magnomechanical platforms, revealing that the predicted chaos regime (microwave driving power $P_{\rm d} = 1$ nW, bias magnetic field $B_0 \sim 0.3$ T, and magnon–phonon dissipative coupling strength $\Gamma/2\pi \leq 20$ MHz) aligns with currently achievable specifications in YIG-based systems.[5,51] Second, purely dissipative coupling between the cavity and magnon modes can be experimentally realized by placing the YIG sphere above the center of the crossline-microwave circuit, and in addition, the dissipative coupling strength can be changed by moving the position of the YIG sphere.[47,48] Third, YIG crystal maintains a good ferromagnetic property at room temperatures as a result of its Curie temperature being as high as 559 K, which means that the dissipative-coupling-induced magnomechanical chaos is robust against thermal noise at room temperature.[62] Finally, the dissipative coupling-induced magnomechanical chaos exhibits inherent compatibility with hybrid quantum systems. Recent advances in nanofabrication techniques have enabled seamless integration of YIG spheres with on-chip architectures, further facilitating their implementation in scalable quantum platforms. Our findings not only confirm the experimental accessibility within state-of-the-art magnonic architectures but also establish a concrete roadmap for implementing chaotic dynamics as a functional resource in hybrid magnonic systems.

3. Conclusion

In summary, we have theoretically demonstrated that dissipative coupling serves as a powerful mechanism to induce magnomechanical chaos with an ultra-low driving threshold in an open cavity magnomechanical system. By introducing dissipative coupling between the magnon and cavity modes, the nonlinear magnetostrictive interaction is significantly enhanced, overcoming the inherent limitation of weak magnetostriction in triggering chaotic dynamics. Numerical simulations reveal that chaotic motion emerges at an unprecedentedly low driving power ($\sim$ nW), accompanied by a positive Lyapunov exponent. The degree of chaos can be precisely tuned by adjusting the dissipative coupling strength, providing a versatile control knob for chaotic dynamics. This work not only deepens the understanding of nonlinear magnomechanics in open systems but also establishes a practical pathway for harnessing chaos in hybrid quantum technologies, such as secure communication and chaotic information transfer.

Acknowledgements

This work was supported by the National Natural Science Foundation of China (Grant No. 12105047) and Guangdong Basic and Applied Basic Research Foundation (Grant No. 2022A1515010446).

References

[1] Chumak A V, Vasyuchka V I, Serga A A and Hillebrands B 2015 *Nat. Phys.* **11** 453
[2] Dany L Q, Yutaka T, Arnaud G, Koji U and Yasunobu N 2019 *Appl. Phys. Express* **12** 070101
[3] Yuan H Y, Cao Y S, Kamra A, Duine R A and Yan P 2022 *Phys. Rep.* **965** 1
[4] Zheng S S, wang Z Y, Wang Y P, Sun F X, He Q Y, Yan P and Yuan H Y 2023 *J. Appl. Phys.* **134** 15
[5] Zhang X, Zou C L, Jiang L and Tang H X 2016 *Sci. Adv.* **2** e1501286
[6] Holanda J, Maior D S, Azevedo A and Rezende S M 2018 *Nat. Phys.* **14** 500
[7] Yu M, Shen H and Li J 2020 *Phys. Rev. Lett.* **124** 213604
[8] Shen Z, Xu G T, Zhang M, Zhang Y L, Wang Y, Chai C Z, Zou C L, Guo G C and Dong C H 2022 *Phys. Rev. Lett.* **129** 243601
[9] Hatanaka D, Asano M, Okamoto H, Kunihashi Y, Sanada H and Yamaguchi H 2022 *Phys. Rev. Appl.* **17** 034024
[10] Hei X L, Li P B, Pan X F and Nori F 2023 *Phys. Rev. Lett.* **130** 073602
[11] Liu Z X, Wang B, Xiong H and Wu Y 2018 *Opt. Lett.* **43** 3698
[12] Xu Y, Liu J Y, Liu W and Xiao Y F 2021 *Phys. Rev. A* **103** 053501
[13] Zhao C S, Yang Z, Peng R, Yang J, Li C and Zhou L 2022 *Phys. Rev. Appl.* **18** 044074
[14] Chen Y T, Du L, Zhang Y and Wu J H 2021 *Phys. Rev. A* **103** 053712
[15] Li J, Zhu S Y and Agarwal G S 2018 *Phys. Rev. Lett.* **121** 203601
[16] Li J, Wang Y P, You J Q and Zhu S Y 2022 *Natl. Sci. Rev.* **10** nwac247
[17] Qiu W, Cheng X, Chen A, Lan Y and Nie W 2022 *Phys. Rev. A* **105** 063718
[18] Hussain B, Qamar S and Irfan M 2022 *Phys. Rev. A* **105** 063704
[19] Li J, Zhu S Y and Agarwal G S 2019 *Phys. Rev. A* **99** 021801
[20] Zhang W, Wang D Y, Bai C H, Wang T, Zhang S and Wang H F 2021 *Opt. Express* **29** 11773
[21] Kong C, Wang B, Liu Z X, Xiong H and Wu Y 2019 *Opt. Express* **27** 5544
[22] Lu T X, Xiao X, Chen L S, Zhang Q and Jing H 2023 *Phys. Rev. A* **107** 063714
[23] Xu G T, Zhang M, Wang Z Y, Liu Y X, Shen Z and Guo G C 2023 *Fundamental Res.* **3** 45
[24] Shen R C, Li J, Fan Z Y, Wang Y P and You J Q 2022 *Phys. Rev. Lett.* **129** 123601
[25] Liu Z X, Xiong H and Wu Y 2019 *Phys. Rev. B* **100** 134421
[26] Liu Z X, Wu Y H and Sun J H 2025 *Front. Phys.* **20** 063200
[27] Zoepfl D, Juan M L, Schneider C M F and Kirchmair G 2020 *Phys. Rev. Lett.* **125** 023601

[28] Kani A, Sarma B and Twamley J 2022 *Phys. Rev. Lett.* **128** 013602
[29] Zoepfl D, Juan M L, Diaz-Naufal N, Schneider C M F, Deeg L F, Sharafiev A, Metelmann A and Kirchmair G 2023 *Phys. Rev. Lett.* **130** 033601
[30] Xiong H 2025 *Sci. China-Phys. Mech. Astron.* **68** 250313
[31] Liu Z X and Li Y Q 2022 *Photon. Res.* **10** 2786
[32] Xiong H 2023 *Fundamental Res.* **3** 8
[33] Liu Z X, Peng J and Xiong H 2023 *Phys. Rev. A* **107** 053708
[34] Xu G T, Zhang M, Wang Y, Shen Z, Guo G C and Dong C H 2023 *Phys. Rev. Lett.* **131** 243601
[35] Potts C A, Varga E, Bittencourt V A S V, Kusminskiy S V and Davis J P 2021 *Phys. Rev. X* **11** 031053
[36] Bittencour V A S V t, Potts C A, Huang Y, Davis J P and Viola Kusminskiy S 2023 *Phys. Rev. B* **107** 144411
[37] Potts C A, Huang Y, Bittencourt V A S V, Viola Kusminskiy S and Davis J P 2023 *Phys. Rev. B* **107** L140405
[38] Lee O, Yamamoto K, Umeda M, Zollitsch C W, Elyasi M, Kikkawa T, Saitoh E, Bauer G E W and Kurebayashi H 2023 *Phys. Rev. Lett.* **130** 046703
[39] Liao Q, Peng K and Qiu H 2023 *Chin. Phys. B* **32** 054205
[40] Amghar M, Chabar N and Amazioug M 2024 *Chin. Phys. B* **33** 120308
[41] Ott E, Grebogi C and Yorke J A 1990 *Phys. Rev. Lett.* **64** 2837
[42] Boccaletti S, Grebogi C, Lai Y C, Mancini H and Maza D 2000 *Phys. Rep.* **329** 103
[43] Crutchfield J P 2012 *Nat. Phys.* **8** 17
[44] Liu Z X, You C, Wang B, Dong H, Xiong H and Wu Y 2020 *Nanoscale* **12** 2118
[45] Peng J, Liu Z X, Yu Y F and Xiong H 2024 *Phys. Rev. A* **110** 053704
[46] Liu Z X, You C, Wang B, Xiong H and Wu Y 2019 *Opt. Lett.* **44** 507
[47] Wang Y P and Hu C M 2020 *J. Appl. Phys.* **127** 130901
[48] Harder M, Yao B M, Gui Y S and Hu C M 2021 *J. Appl. Phys.* **129** 201101
[49] Harder M, Yang Y, Yao B M, Yu C H, Rao J W, Gui Y S, Stamps R L and Hu C M 2018 *Phys. Rev. Lett.* **121** 137203
[50] Xu P C, Rao J W, Gui Y S, Jin X F and Hu C M 2019 *Phys. Rev. B* **100** 094415
[51] Yang Y, Wang Y P, Rao J W, Gui Y S, Yao B M, Lu W and Hu C M 2020 *Phys. Rev. Lett.* **125** 147202
[52] Yu W C, Wang J J, Yuan H Y and Xiao J 2019 *Phys. Rev. Lett.* **123** 227201
[53] Yang Y, Rao J W, Gui Y S, Yao B M, Lu W and Hu C M 2019 *Phys. Rev. Applied* **11** 054023
[54] Zhao C S, Yang Z, Peng R, Yang J Y, Li C and Zhou L 2022 *Phys. Rev. Appl.* **18** 044074
[55] Wang Y M, Xiong W, Xu Z Y, Zhang G Q and You J Q 2022 *Sci. China-Phys. Mech. Astron.* **65** 260314
[56] Nair Mukhopadhyay J M P D and Agarwal G S 2021 *Phys. Rev. Lett.* **126** 180401
[57] Nair J M P, Mukhopadhyay D and Agarwal G S 2021 *Phys. Rev. B* **103** 224401
[58] Pan H, Yang Y, An Z H and Hu C M 2022 *Phys. Rev. B* **106** 054425
[59] Liu Z X 2024 *Appl. Phys. Lett.* **124** 032403
[60] Van Wiggeren G D and Roy R 1998 *Science* **297** 1198
[61] Argyris A, Syvridis D, Larger L, Annovazzi-Lodi V, Colet P, Fischer I, García-Ojalvo J, Mirasso C R, Pesquera L and Shore K A 2005 *Nature* **438** 343
[62] Serga A A, Chumak A V and Hillebrands B 2010 *J. Phys. D* **43** 264002
[63] Liu Z X, Zuo X J, Peng J X and Xiong H 2026 *Appl. Phys. Rev.* **13** 011307
[64] Clerk A A, Devoret M H, Girvin S M, Marquardt F and Schoelkopf R J 2012 *Rev. Mod. Phys.* **82** 1155
[65] Wang Z Y, Qian J, Wang Y P, Li J and You J Q 2023 *Appl. Phys. Lett.* **123** 153904
[66] Yao B, Gui Y S, Rao J W, Zhang Y H, Lu W and Hu C M 2023 *Phys. Rev. Lett.* **130** 146702